

Fulde-Ferrel-Larkin-Ovchinnikov phase in a one-dimensional Fermi gas with attractive interactions and transverse spin-orbit coupling

Monalisa Singh Roy^{1,2,*} and Manoranjan Kumar^{2,†}

¹*Department of Physics, Bar-Ilan University, Ramat Gan 52900, Israel*

²*S. N. Bose National Centre for Basic Sciences, Block - JD, Sector - III, Salt Lake, Kolkata 700106, India*

 (Received 31 August 2023; revised 14 May 2024; accepted 23 May 2024; published 28 August 2024)

We examine the existence and characteristics of the exotic Fulde-Ferrel-Larkin-Ovchinnikov (FFLO) phase in a one-dimensional Fermi gas with attractive Hubbard interactions in the presence of spin-orbit coupling (SOC) and Zeeman field. We show that a robust FFLO phase can be created in the presence of attractive on-site interactions and Zeeman field, and that the addition of SOC suppresses the FFLO order and enhances the pair formation. In the absence of SOC, the system shows four phases: Bardeen-Cooper-Schrieffer (BCS), FFLO, multimode pairing, and fully polarized phases by tuning the Zeeman field h . The quantum transition between these phases is discontinuous with respect to h . In the presence of SOC, the transition from the BCS to FFLO phase becomes continuous. We present a complete phase diagram of this model both in the presence and in the absence of SOC at a quarter electron filling and also explore the effect of SOC on the FFLO phase.

DOI: [10.1103/PhysRevB.110.085159](https://doi.org/10.1103/PhysRevB.110.085159)

I. INTRODUCTION

The presence of external magnetic and electric fields in superconducting materials give rise to many exotic phases, and their effects have been extensively studied [1,2] since the discovery of superconductivity in 1911 [3]. Over the years, discovery of superconducting materials and improvements in their synthesis mechanism have yielded steadily increasing superconducting transition temperatures (T_c) [4] and more refined applications of superconducting materials in daily life [5]. At high temperatures, strong magnetic field h destroys the superconducting properties in materials [6], whereas at low temperatures and low to moderate magnetic fields, these materials give rise to many exotic phenomena like the Meissner effect [7], vortex formations [8,9], Fulde-Ferrel [10] (FF), and Larkin-Ovchinnikov [11] (LO) phases etc. In Bardeen-Cooper-Schrieffer (BCS) superconductors [12], electrons of opposite spins and momenta form Cooper pairs. However, in the presence of low h , the Fermi energies of (up spin and down spin) electrons shift and the electron pairing process gets affected. Fulde and Ferrel [10], and Larkin and Ovchinnikov [11] independently showed that in presence of magnetic field, a robust superconducting order could coexist with a magnetic order in superconductors, and electron pairs with nonzero momentum can be formed in an inhomogeneous superfluid phase [13]. Since then, there has been much effort to realize this phase in various materials [14], especially in layered superconductors like $\text{La}_{2-x}\text{Ba}_x\text{CuO}_4$ [15], CeCoIn_5 [16], and organic salts like BEDT – TTF [17]. However, this phase is fragile since any impurity or other perturbations can disturb this phase in materials [18–20].

In recent years, cold atoms confined in optical lattices have emerged as an excellent alternative playground to explore superconductivity in pristine conditions—to study different pairing mechanisms in it and effects of various external fields on the superconducting state [21]. The existence of Bose-Einstein condensation (BEC) was demonstrated in a gas of cooled sodium (Na) atoms by Davis *et al.* in 1995 [22]. Since then, existence of superfluidity has been realized in various Fermi and Bose gases [23–27]. The physics of these gases trapped in optical lattices are well described by Hubbard-like models with effective on-site interactions $U < 0$ that are created by tuning Feshbach resonance in the system [28]. Synthetic spin-orbit coupling (SOC) and Zeeman fields are created through Raman coupling [29,30]. One-dimensional (1D) Fermi gas with attractive interactions shows a BEC phase at very strongly attractive interactions, and a BCS phase with s -wave-like pairings for moderate U [31]. Introduction of Zeeman field h in this system takes the system from a BCS phase at a low h , to a partially polarized phase at moderate h , and a fully polarized (FP) phase for high h [32–34]. This partially polarized phase at moderate h is proposed to host exotic pairing, like Fulde-Ferrel-Larkin-Ovchinnikov (FFLO) phase [10,11]. This phase is characterized by finite momentum of the center of mass of bound pairs, which is reflected in the twin peaks (at $\pm k$) in the pair density correlations in momentum space.

The FFLO phase is more stable in 1D systems due to the absence of eddy currents and phase separations, which are more common in three-dimensional (3D) systems and make it difficult for 3D systems to host the FFLO phase [13]. In addition, the 1D FFLO phase is expected to host the nontrivial p -wave-like pairings in the presence of a transverse SOC field [35,36]. This phase is also proposed to host topological edge modes whose hallmarks are reported to be exponentially decaying energy gaps as a function of increasing system size [37,38]. There are many studies of model Hamiltonians,

*Contact author: singhroy.monalisa@gmail.com;
monalisa12i@bose.res.in

†Contact author: manoranjan.kumar@bose.res.in;
manoranjan15@gmail.com

ranging from simple Fermi Hubbard models with additional interaction terms to systems with proximity-induced superconducting terms, for exploring the existence of the FFLO phase. Lüscher *et al.* studied 1D attractive Hubbard model in the presence of finite spin polarization and showed the existence of the FFLO phase and its fingerprint in spatial noise correlations [39]. Yang used a field theoretic approach to study the nonuniform superconducting states in quasi-1D systems and plotted a schematic phase diagram in the phase space of Luttinger liquid parameter K and magnetic field h [40]. Rizzi *et al.* also studied the attractive Hubbard model to study the stability of the FFLO phase in optical lattices [41]. Feiguin *et al.* studied this model with confining parabolic potential in the optical lattice [34]. Most of these works focused on systems with actual or induced superconducting order parameters, which yield BCS and FFLO phases with long-range orders. However, similar studies are scant in the context of electron number conserving systems, especially in the presence of both magnetic and SOC fields, which as already mentioned, are expected to host nontrivial p -wave pairing and possible topological phases [35–37]. In these systems, the BCS, and FFLO phases are expected to show quasi-long-range correlations and no true long-range correlations, in accordance with the Mermin-Wagner theorem [42]. In such a system, the superconducting order parameter vanishes in the thermodynamic limit, and density pair correlations are used to instead characterize the different phases [13,33,41]. In this paper, we present systematic theoretical studies of a quantum phase diagram of the 1D attractive Fermi gas model Hamiltonian subjected to Zeeman field and an SOC field, as a function of on-site interactions U , and show the emergence of various exotic quantum phases, including one with FFLO pairings, as characterized by the pair-density correlations.

In this paper, we study a simple model of 1D Fermi gas in the limit of attractive on-site interaction ($U < 0$) to explore the FFLO phase and associated phase transitions at low filling fraction $\nu = 0.25$. We study this system both (i) in the absence of SOC and (ii) in the presence of a transverse SOC. We find that the FFLO phase spans a large area of the phase diagram for all electronic densities, both in the absence and presence of SOC. We present a complete phase diagram of this model in the phase space of U and h and for SOC strengths $\alpha = 0$ and 0.05.

The paper is organized into four sections. In Sec. II, we introduce the model and the numerical technique. In Sec. III, we discuss the main criteria used for identifying the FFLO phase in the system. We first focus on the case with no SOC and discuss the different phases in the $h - U$ parameter space of the system. Next, we add a transverse SOC field (in the x direction) and explore its effect on the FFLO phase. We conclude with a brief discussion of the reported results and their possible impact on the current understanding of exotic pairings in 1D ultracold systems and implications thereof in Sec. IV.

II. MODEL AND METHOD

We study the 1D Fermi gas with attractive on-site interactions U in the presence of a Zeeman field h and transverse

SOC field α . The model Hamiltonian of this system can be written as

$$H = H_t + H_U + H_Z + H_{\text{SOC}}, \quad (1)$$

where

$$\begin{aligned} H_t &= -t \sum_{i,\sigma} (C_{i,\sigma}^\dagger C_{i+1,\sigma} + \text{H.c.}), \\ H_U &= U \sum_i n_{i,\uparrow} n_{i,\downarrow}, \quad H_Z = -h \sum_i S_i^z, \\ H_{\text{SOC}} &= +i\alpha \sum_i (C_{i,\uparrow}^\dagger C_{i+1,\downarrow} + C_{i,\downarrow}^\dagger C_{i+1,\uparrow} - \text{H.c.}), \end{aligned}$$

where $C_{i,\sigma}^\dagger$ ($C_{i,\sigma}$) are creation (annihilation) operators and $n_{i,\sigma}$ is the number operator at site i , with $\sigma = \uparrow$ up spin or \downarrow down spin. We set $t = 1$ to define the energy scale for our calculations. We study the system away from the half-filling limit and in the attractive interaction regime $U \in [-1, -4]$. The quantity $\nu = n/2N$ defines the filling fraction of a system of N sites containing n electrons. In the absence of U and α , the spin-up and spin-down electronic bands split in the presence of the external magnetic field h . An attractive U induces intraband pairing correlations, whereas a transverse SOC generates spin-momentum locking along the x axis of the system, thus giving rise to a p -wave-like pairing [43].

We have used a state-of-the-art density matrix renormalization group (DMRG) method for solving the Hamiltonian in Eq. (1). It is a versatile numerical technique for accurately calculating the low-lying eigenvalues and eigenvectors of various low-dimensional many-body systems [44–50]. It is based on the systematic truncation of irrelevant degrees of freedom at every step of the infinite and finite DMRG algorithms. In the fermionic system under study, the spin degrees of freedom are not conserved, hence the density matrix (Hamiltonian) dimension is significantly large. The eigenvectors of the density matrix of the system block corresponding to $m \simeq 700$ largest eigenvalues have been retained to maintain a reliable accuracy. More than ten finite DMRG sweeps have been performed for each calculation to minimize the error in per site energies to less than 1% and the maximum system size studied is $N = 120$.

III. RESULTS

In this section, we present the numerical studies investigating the existence of a robust FFLO phase in 1D ultracold atoms with intrinsic attractive on-site interactions and Zeeman field, first in the absence of SOC and then in presence of a transverse SOC field in the x direction. Most of the results presented in this paper are for the quarter-filling fraction $\nu = 0.25$, however, we found that the FFLO phase exists for a wide range of densities. We also present a quantum phase diagram of the model in $h - U$ parameter space for $\nu = 0.25$ and study the effect of finite SOC interactions $\alpha > 0$ on the FFLO phase. We show that a robust FFLO phase exists for a wide range of electron fillings U , h , and α , and this phase is distinct from other phases like the BCS and a multimode pairing (MMP) phase, which appears just before the system transitions into a FP phase at high h .

To characterize various phases in the system we study the pair density correlations or singlet pair correlation function $P(i, j)$ and its Fourier transform (FT). The singlet pair correlation is defined as

$$P(i, j) = \langle C_{i\uparrow}^\dagger C_{i\downarrow}^\dagger C_{j\uparrow} C_{j\downarrow} \rangle. \quad (2)$$

Its FT of $P(i, j)$ is given by

$$P(k) = \sum_k e^{-ik \cdot r_{ij}} P(i, j), \quad (3)$$

where $(r_{ij} = i - j)$, and i, j represent site indices in the system. The single peak in $P(k)$ at $k = 0$ indicates that the electron pairs are formed at zero momentum, i.e., opposite electronic spins undergoing pair formation at $k = 0$, which is a signature of quasiparticles in the BCS phase. Twin peaks at finite momenta in the $P(k)$ momentum distribution curve are a hallmark of an underlying FFLO-like pairing where electrons with opposite spins form pairs with a net nonzero momentum. In a mixed BCS-FFLO phase, where both the conventional BCS phase and the FFLO phase coexist, $P(k)$ shows three peaks: one at zero momentum $k = 0$ and twin peaks at a finite momentum k_h . At sufficiently high magnetic field, $P(i, j)$ is short-ranged in nature, and $P(k)$ shows two peaks at $\pm k_h$ and a nonzero constant plateau of $P(k)$ between these two maxima, i.e., all the momenta between $\pm k_h$ contribute towards the pair formation. We call this phase the MMP phase. Thereafter, at even higher magnetic field the system transitions into a fully polarized phase; $P(k)$ is zero. We also study two energy gaps—the pair-binding energy (E_b) or the parity gap, and the excitation energy gap Δ , defined as

$$E_b(n, N) = \frac{1}{2}[E_0(n+1, N) + E_0(n-1, N) - 2E_0(n, N)], \quad (4a)$$

$$\Delta(n, N) = E_1(n, N) - E_0(n, N), \quad (4b)$$

where $E_0(n, N)$ and $E_1(n, N)$ represent the ground-state energy and the first excited-state energy, respectively, with n electrons in the system of N sites. The finite binding energy E_b is the signature of the BCS phase, whereas the exponential decay of $\Delta(n, N)$ may indicate the existence of a topological phase.

The other calculated quantities include local charge density with up spin $n_\uparrow(i)$, down spin $n_\downarrow(i)$, and local spin density $S^z(i)$. We notice that the spatial distributions of these quantities are different for each of the observed phases. In the BCS phase, $n_\uparrow(i)$ and $n_\downarrow(i)$ have an overlapping spiral nature. For the partially polarized phases, FFLO and MMP, $n_\uparrow(i)$ and $n_\downarrow(i)$ are separated and a difference in the wavelength or pitch angle of the spiral oscillations is observed.

A. In absence of SOC

In the absence of any magnetic field, the system remains in the trivial BCS phase, which is characterized by quasiparticle pairs with zero net momentum. In the presence of a finite magnetic field h , the system can transition into the FFLO phase, where the electron pairs are formed with net nonzero momentum due to the population imbalance between the up and down spins created by the magnetic field. This phase is expected to retain quasi-long-range correlations, especially in

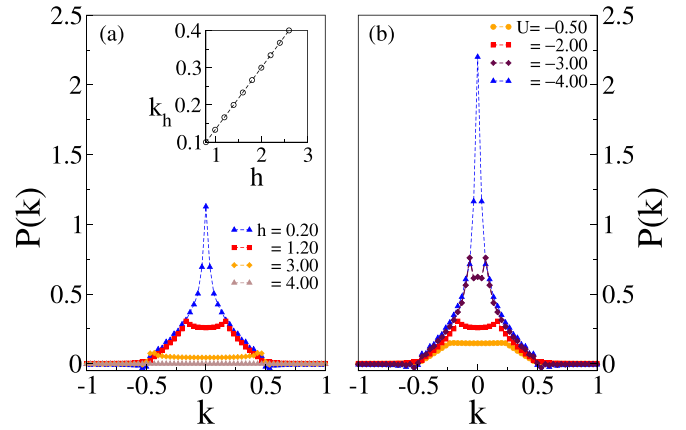


FIG. 1. FT of singlet pair density correlations, $P(k)$ vs k for (a) different $h = 0.20, 1.20, 3.00,$ and 4.00 , at $U = -2.00$ and for (b) different $U = -0.50, -2.00, -3.00,$ and -4.00 , at $h = 1.20$ for $\nu = 0.25, \alpha = 0$. The inset within (a) shows that the finite momentum, k_h , varies linearly a function of h for $U = -2.00$, and $N = 60$.

1D. To ascertain that, in Fig. 1 the FT of singlet-pair density correlations, $P(k)$ vs k , are plotted for different h and U , for $\nu = 0.25$ and in absence of SOC, i.e., $\alpha = 0$. It shows a single peaked structure at $k = 0$ at low h , as expected from a trivial BCS phase. Increasing h , a two-peaked $P(k)$ with maxima at $\pm k_h$ are observed, indicating the presence of an FFLO phase. In the FP phase at high h , $P(k)$ is vanishingly small and no peak is observed in $P(k)$. Between the FFLO and FP phase, there exists a narrow regime of the MMP phase. In this phase, $P(k)$ shows a plateaulike structure between the twin peaks, i.e., $P(k)$ is uniformly distributed between the momenta $\pm k_h$, which indicates that the momentum of center of mass of the condensate is distributed between $\pm k_h$ around the Fermi momentum. $P(i, j)$ is a fast and algebraically decaying function and the pairing is short-ranged in this phase. The peak height of $P(k)$ is significantly smaller in this phase as compared to the FFLO phase.

In Fig. 1(a), variations of $P(k)$ for four values of h are shown for $U = -2.00$. In Fig. 1(b), the magnetic field $h = 1.20$ is kept fixed and $P(k)$ is plotted for four values of U . A larger value of $|U|$ increases binding energy, therefore, the BCS phase is favored at a higher magnitude of U , and FFLO-like pairing is observed at weakly attractive U at comparatively lower to intermediate values of h (scaled with $t = 1$). For larger $|U|$, a larger magnetic field is required to break the bound electron pairs, hence we notice that $U = -0.50$ is already in the FP state for the given h (Fig. 1). The inset in Fig. 1 shows that the finite momentum of pairing k_h varies linearly with h through the FFLO and MMP phases, as expected, whereas for $U = -4.00$, the BCS phase remains intact up to a large h . We also plot the peak height of $[P_{\max}(k)]$ as a function of h for $U = -2.00$ in Fig. 2, and find that the four phases in this system can be easily identified by the respective plateaus in $[P_{\max}(k)]$ corresponding to each phase. We also notice that the transition from one phase to the other occurs through discontinuous jumps, with increasing h . We plotted $[P_{\max}(k)]$ as a function of $1/N$ in the inset of Fig. 2 and notice that the effect of the finite size is weak in the FFLO and MMP

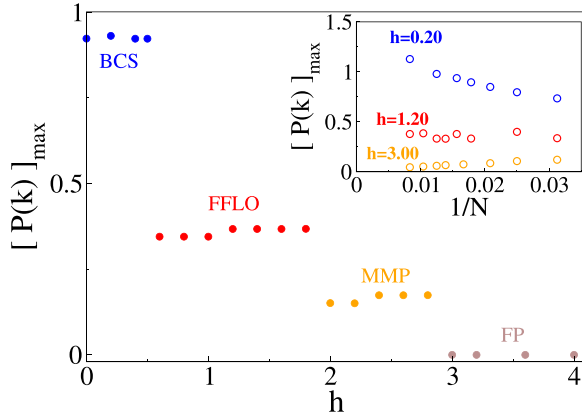


FIG. 2. The maxima of FT of singlet pair density correlations, $[P(k)]_{\max}$ as a function of h at $U = -2.00$, $\nu = 0.25$, and $\alpha = 0$. Inset: $[P(k)]_{\max}$ as a function of inverse system size $1/N$ for different h at $U = -2.00$, $\nu = 0.25$, and $\alpha = 0$.

phases, but $[P_{\max}(k)]$ increases with the system size in the BCS phase.

For further understanding of the different phases, the behavior of local charge and spin densities are analyzed for three values of magnetic field $h = 0.20$, 1.20 , and 3.00 , corresponding to the three phases BCS, FFLO, and MMP, respectively, at $U = -2.00$. Here we have omitted the fully polarized regime where all spins are polarized along the direction of magnetic field h and the charge is uniformly distributed, which is fairly easy to understand and is expected at high h . Figure 3 shows the spatial profile of the spin densities $n_{\sigma}(i)$ and local magnetization, $S^z(i) = n_{\uparrow}(i) - n_{\downarrow}(i)$, for different h . At low $h = 0.20$ [Fig. 3(a)], the up- and down-spin densities overlap and the system is in a trivial BCS phase, which is a non-magnetic state. Above a threshold magnetic field h_{c1} , some of the singlet pairs are broken, leading to a partial magnetic polarization $S^z(i) \neq 0$ in the system as shown in Figs. 2(b) and 2(c). The charge-density wave oscillations have a maximum amplitude for low $h = 1.20$ [Fig. 3(a)] and its amplitude

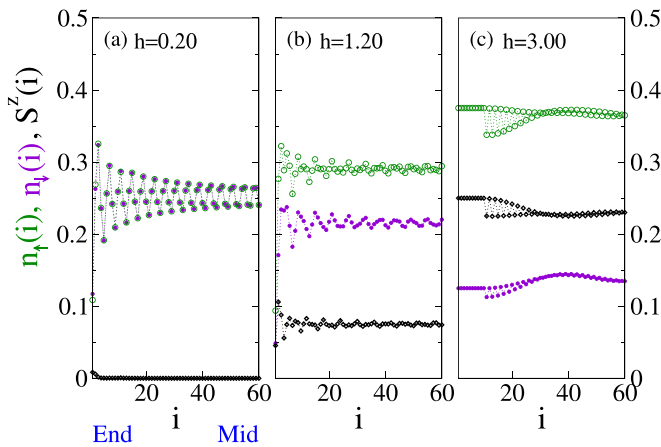


FIG. 3. Spatial profile of local up-charge density $n_{\uparrow}(i)$, local down-charge density $n_{\downarrow}(i)$, and local spin density $S^z(i)$ at (a) $h = 0.20$, (b) $h = 1.20$, and (c) $h = 3.00$ for $U = -2.00$, $\nu = 0.25$, $\alpha = 0$, and $N = 120$.

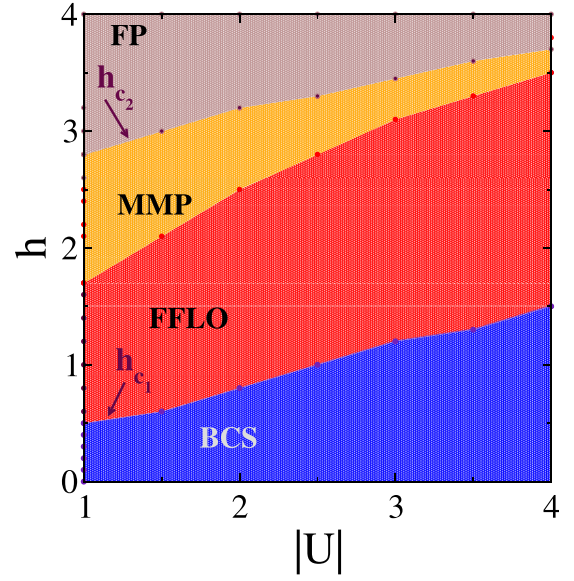


FIG. 4. Phase diagram of the model described by Eq. (1) in the phase space of magnetic field h and on-site attractive interactions, $|U|$, at $\alpha = 0$ and $\nu = 0.25$.

decreases with increasing h [Figs. 3(b) and 3(c)]. At $h = 3.00$ [Fig. 3(c)], the system is in the MMP phase and the density modulations vanish at the middle of the chain. Above another threshold value of magnetic field h_{c2} , the system transitions from the MMP phase to the FP phase. Figure 9 in the Appendix shows that the dominant interactions are s wave in the BCS phase, triplet p wave in the FFLO phase, and of competing s -wave, singlet, and triplet p -wave types, as expected from the mean-field predictions for a spin-imbalanced system with SOC interactions.

Further analyzing the oscillations in the local charge density, we find that at low h , where the system is in a BCS phase, oscillations in $n_{\sigma}(i)$ are described by a sinusoidal function with its amplitude decaying from the edges towards the center. The functional form of $n(i)_{\sigma}$ in this regime is given by $A \sin(\gamma x + A_0) x^{-\eta} + C$. The charge density profile does not change appreciably with increasing h in the BCS phase. For $h > h_{c1}$, another sinusoidal length scale sets in for the partially polarized phases—FFLO and MMP phases—and $n(i)$ can be fitted with the charge density profile: $A \sin(\gamma x + A_0) \sin(\beta x + B_0) x^{-\eta} + C$. The power-law exponent remains $\eta \sim 1$ for all $h < h_{c2}$. Whereas the wavelength of one of the sinusoidal function $\lambda_2 = \frac{2\pi}{\beta}$ decreases with increasing h , the wavelength of the other sinusoidal function $\lambda_1 = \frac{2\pi}{\gamma}$ does not vary with h in the FFLO phase. In the MMP phase, the wavelength $\lambda_2 = \frac{2\pi}{\beta}$ becomes very large, whereas the other wavelength $\lambda_1 = \frac{2\pi}{\gamma}$ decreases significantly to approximately $\sim 2 - 4$ lattice units.

In Fig. 4, we present the quantum phase diagram of the model Hamiltonian described by Eq. (1), in the absence of SOC ($\alpha = 0$) and for $\nu = 0.25$, based on information extracted from $P(k)$, their maxima, charge- and spin-density profiles. All the phase boundaries are based on the $N = 96$ system size and we note that the finite-size scaling of the boundary is very weak, meaning that smaller system sizes

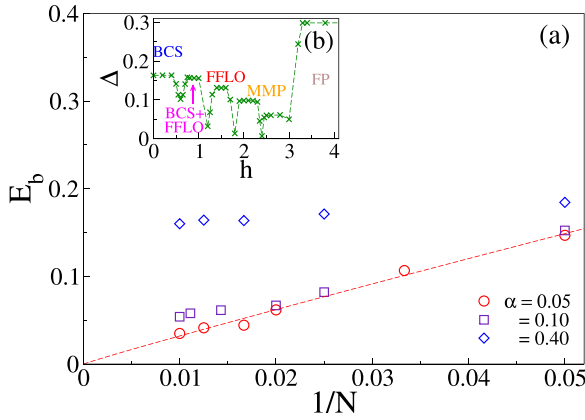


FIG. 5. Binding energy as function of N for different α at $U = -1.00$, $\nu = 0.25$, and $h = 1.00$. Inset: First excitation energy gap Δ as a function of h for $\alpha = 0.05$ at $U = -1.00$ and $\nu = 0.25$

are also sufficient to predict phase boundaries accurately. In the absence of any h , the BCS phase is observed for all values of $|U|$. Upon increasing h , the system goes from a BCS phase to the partially polarized FFLO phase, then from the FFLO phase to the MMP phase, and finally to the FP phase at high h . The FFLO phase is a dominant phase in the quantum phase diagram and the width of this phase increases with $|U|$. The magnetic field required for the transition from the BCS to the FFLO phase, h_{c1} , is smooth and linear with $|U|$. Similarly, the h required for the FFLO to the MMP phase transition also varies linearly with $|U|$, especially in the small $|U| < 2.5$ limit. We also explored the quantum phase diagram at lower fillings ν (the lowest filling studied was $\nu = 0.10$) and found that the phase boundaries shift towards lower h , i.e., slope of the h_c curves increases with decreasing electron filling $\nu < 0.25$. This is because, at lower densities, lower h is sufficient to break the bound pairs in the system.

B. In presence of SOC

In this section, we explore the effect of small SOC strength $\alpha = 0.05$, which is expected to produce a phase similar to p -wave pairing in a superconducting phase for attractive U interactions. This exotic p -wave-like phase is proposed to host topological edge modes [36,51], which is important for applications in quantum computation. One way of distinguishing phases in the presence of SOC is the binding energy, defined in Eq. (4a). In the superconducting BCS state, the binding energy of the system should be finite, whereas in the FFLO, the MMP and the FP phase unpaired electron should have zero binding energy.

The binding energy is plotted as a function of system size N in Fig. 5 for different $\alpha = 0, 0.05, 0.10$, and 0.40 at $\nu = 0.25$, at $h = 1$. We find that E_b vanishes algebraically with N for low α , which corresponds to the FFLO phase. For higher α , the system goes to the BCS phase and E_b has a finite value in the thermodynamic limit. The inset of Fig. 5 shows the variation of the lowest excitation energy gap Δ with h . The inset of Fig. 5 shows fluctuations at the phase boundaries of the $\Delta - h$

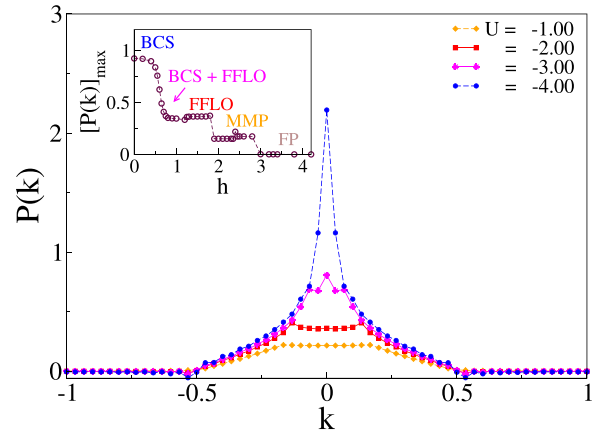


FIG. 6. FT of singlet pair density correlations, $P(k)$ vs k for different U , at $h = 1.00$, $\nu = 0.25$, $\alpha = 0.05$. Inset: The maxima of FT of singlet pair density correlations, $[P(k)]_{\max}$ as a function of h , at $U = -2.00$, $\nu = 0.25$, and $\alpha = 0.05$.

plot for a given system size. The fluctuations at the boundary can be utilized to determine the phase boundaries and we notice that the boundaries determined by this method agree well with those indicated by the pair correlation structure factor $P(k)$ in Fig. 6.

$P(k)$ vs k is now plotted in Fig. 6 for four values of U at $h = 1.00$, $\alpha = 0.05$, and $\nu = 0.25$. The FFLO pairings are observed for weakly attractive U , as indicated by the twin peaks in $P(k)$ for $U = -1.00$ and -2.00 , whereas a single peaked $P(k)$ is observed for stronger $U = -4.00$, indicative of a BCS phase. At $U = -3.00$, a three-peaked structure is observed, which is a signature of an exotic mixture of BCS and FFLO phases. It should be noted that this exotic mixture state is not observed for any value of h and U in the absence of α , i.e., a finite SOC field of the form described in Eq. (1) creates this mixture state. $[P(k)]_{\max}$ is plotted as a function of h as shown in the inset of Fig. 6. Contrasting with the inset of Fig. 2, we find that the transition from the BCS to FFLO phase now shows a smooth transition from the BCS phase to the FFLO state through a mixed BCS-FFLO phase. This BCS phase to FFLO phase transition was earlier discontinuous in the absence of SOC ($\alpha = 0$). The transition from the FFLO to MMP phase and from the MMP to FP phase remains discontinuous with increasing h , as before.

To understand the effect of α on the system, we study the $P(k)$ vs k characteristics for different strengths of α in Fig. 7. We find that the FFLO phase is retained at low α [Figs. 7(a) and 7(b)], and the BCS phase sets in for higher α [Figs. 7(d) and 7(e)] for a fixed h . For intermediate α [Fig. 7(c)], a mixed FFLO-BCS phase is observed.

A quantum phase diagram of this system for a fixed $\alpha = 0.05$ is shown in Fig. 8 based on various criteria. It shows that in the absence of h , the BCS phase is observed for all attractive U . Upon increasing h , the system goes from first an unpolarized BCS phase to a partially polarized FFLO phase continuously, through a mixed BCS-FFLO phase which was earlier not observed in the absence of an SOC field (Fig. 4). The width of the BCS phase and FFLO phase shrinks in the

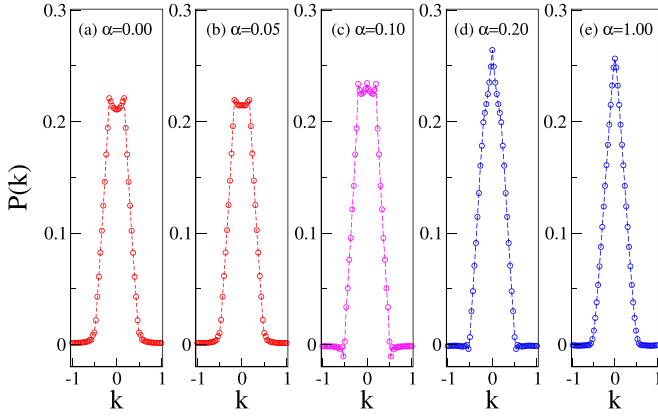


FIG. 7. FT of singlet pair density correlations, $P(k)$ vs k for different α at $h = 1.00$, $\nu = 0.25$, $U = -1.00$.

presence of the SOC. Thereafter, increasing h the system goes from the FFLO to the MMP phase. The width of the MMP phase increases in the large $|U|$ limit, in the presence of SOC. Further enhancing h leads to the FP phase, and the width of this phase increases in smaller $|U|$ in the presence of SOC. We checked that a similar phase diagram is observed for lower fillings $\nu \in [0.10, 0.25]$ as well, except that the phase boundaries are shifted towards lower h , but the qualitative behavior and sequence of the phases remains the same. The phase diagram also remains qualitatively the same for higher α , however, the phase boundaries are shifted towards higher h .

IV. DISCUSSION AND CONCLUSION

In this paper, we studied the 1D Fermi gas model with its Hamiltonian described by Eq. (1), including attractive

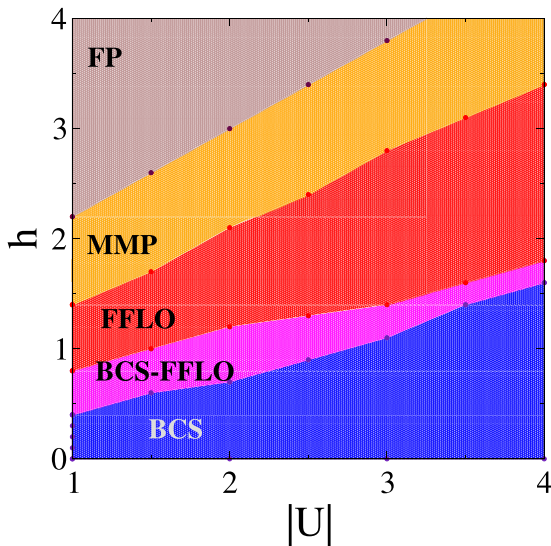


FIG. 8. Phase diagram of the model described by Eq. (1) in the phase space of magnetic field h and on-site attractive interactions, $|U|$, at $\alpha = 0.05$ and $\nu = 0.25$.

on-site interactions, $-|U|$, SOC field, parametrized by α , and a Zeeman field, h . We explored the existence and signatures of the exotic FFLO phase in this system. While extensive literature exists for the FFLO phase, especially in the context of superconducting systems [14], we have focused on studying the FFLO phase in an electron-number conserving model, realizable via cold atomic gases. Also, the attractive interactions considered are just on-site Hubbard interactions tuned by $-|U|$ and do not include actual superconducting correlations.

We presented the quantum phase diagram of this Fermi gas model in the $h - |U|$ parameter space, both in the absence and presence of the SOC field, at electron filling $\nu = 0.25$. Most of the earlier works explored the FFLO phase in a 1D system at $\nu = 0.50$ [33] and $\nu = 0.25$ [52] and restricted their studies to just characterizing the FFLO phase [13]. We have found the quantum phase diagram of this model [Eq. (1)] in the phase space of $h - |U|$ for different α and provided different criteria to identify the phases observed in this system, including the different partially polarized phases at $\nu = 0.25$. We note that the sequence of phases are the same for lower fillings as well, at least up to $\nu = 0.10$.

We found that on-site interactions $U < 0$ and SOC interactions α promote BCS pairings, whereas the Zeeman field h promotes the FFLO order in the system. In the $h - |U|$ phase space, we found four different phases: (i) the BCS phase at low h , (ii) the FFLO phase, (iii) the MMP phase at intermediate h , and (iv) the FP phase at high h . In the trivial BCS phase, singlet quasiparticle pairs are formed (indicated by a single peaked structure at $k = 0$ in the FT of the pair density correlations, Fig. 1), and they show charge density oscillations at low h , low α , and weak U . In the exotic FFLO and MMP phases, there exist commensurate charge and spin oscillations at moderate h , moderate U , and moderate α . The FFLO phase is characterized by quasi-long-range order in the system and correlated singlet pairs with finite momenta [40]. In the FFLO phase, the pair density correlations, $P(r)$, have modulated quasi-long-range order with a single wavelength, which is reflected through twin peaks in the FT of singlet pair density correlations in the system at $\pm k_h$. We also reported a quantum MMP at higher h in which the pair density correlations, $P(r)$, have a short-range order and its FT gives a constant plateau between $\pm k_h$. It is very different from the FFLO phase where $\pm k_h$ are sharply defined. As expected, k_h varies linearly with h , in both the FFLO and MMP phases. Figure 9 in the Appendix studies various pair correlations in the systems and confirms that in the FFLO phase, p -wave correlations are the most dominant, whereas the BCS wave is dominated by s -wave correlations in the system. We observed these phases both in the absence and presence of the SOC field, and the FFLO phase occupies a large area of the quantum phase diagram. In the presence of SOC, a mixed state exhibiting both BCS and FFLO pairings is also observed. The phase diagram of the system remains similar for lower electronic fillings $\nu \in [0.10, 0.25]$, except that the phase boundaries shift to lower h for lower ν . The phase boundaries shift to higher h for higher α , but qualitatively remains the same.

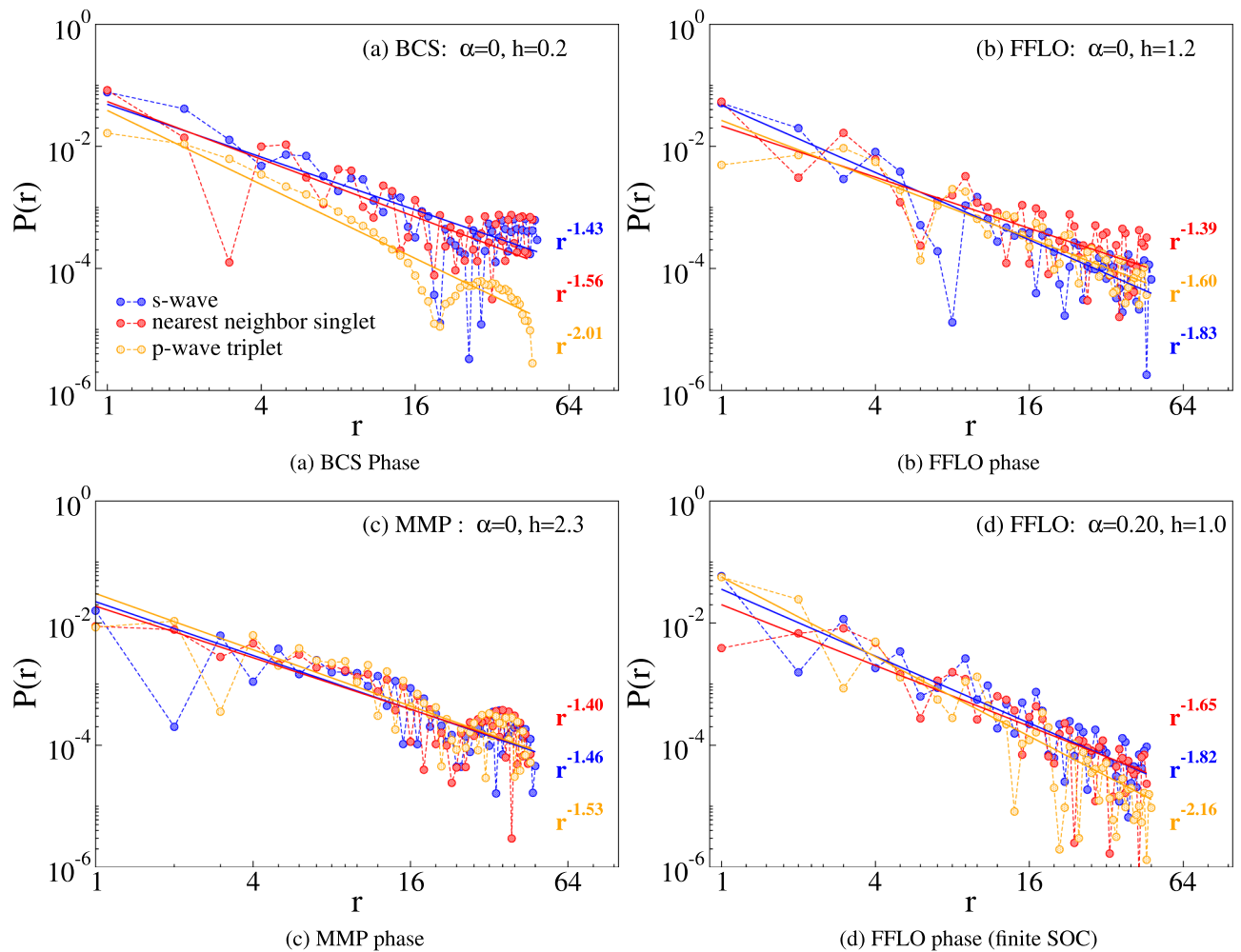


FIG. 9. The following pair correlations, $P(r)$, in various phases of the system are plotted: (i) s wave (blue), (ii) nearest-neighbor singlet (red), and (iii) p -wave triplet (yellow) at (a) $\alpha = 0$ and $h = 0.20$, (b) $\alpha = 0$ and $h = 1.20$, (c) $\alpha = 0$ and $h = 2.30$, and (d) $\alpha = 0.20$ and $h = 1.00$ for $N = 96$, $U = -1$, and $\nu = 0.25$ electronic filling.

In summary, this paper presents a comprehensive study of the quantum phase diagram of a 1D Fermi gas system with intrinsic attractive on-site interactions, a Zeeman field, and transverse SOC, and discusses in detail various methods of characterizing these phases in similar 1D Fermi gas systems. We showed that the FFLO phase dominates the phase diagram and is robust even in the presence of the SOC. This could have potential applications in understanding the unconventional superconductivity phases in low-dimensional electron gas. This model can be easily implemented in trapped cold atoms in optical lattices, and the parameter values used for each of the fields in the Hamiltonian (1) is well within experimental reach.

ACKNOWLEDGMENTS

M.S.R. and M.K. thank S. Saha for help with a part of numerics. M.S.R. thanks Prof. F. Heidrich-Meisner for discussion. M.K. thanks SERB for financial support through Grant Sanction No. CRG/2020/000754.

APPENDIX: COMPARISON OF DIFFERENT PAIR DENSITY CORRELATIONS

This Appendix provides more details regarding the underlying correlations in various phases of the system. We have numerically calculated various pair correlations, $P(r = |i - j|) = \Delta_j^\dagger \Delta_i$ in the system, as described below:

- (i) s -wave correlations, $\Delta_j^\dagger = \langle c_{j,\downarrow}^\dagger c_{j,\uparrow}^\dagger \rangle$,
- (ii) nearest-neighbor singlet correlations, $\Delta_j^\dagger = \langle c_{j,\downarrow}^\dagger c_{j+1,\uparrow}^\dagger - c_{j,\uparrow}^\dagger c_{j+1,\downarrow}^\dagger \rangle$, and
- (iii) p -wave triplet correlations, $\Delta_j^\dagger = \langle c_{j,\downarrow}^\dagger c_{j+1,\uparrow}^\dagger + c_{j,\uparrow}^\dagger c_{j+1,\downarrow}^\dagger \rangle$.

$i = \frac{N}{2}$ has been kept fixed in our calculations. We see from Fig. 9 that the s -wave correlations are dominant in the BCS phase [Fig. 9(a)], whereas the p -wave (triplet) and nearest-neighbor singlet correlations dominate in the FFLO [Figs. 9(b) and 9(d)] and the MMP [Fig. 9(c)] phases, as expected. In the MMP phase, we find that all the correlations are of competing order and are mixed.

- [1] M. N. Wilson, *IEEE Trans. Appl. Supercond.* **22**, 3800212 (2012).
- [2] P. A. Abetti and P. Haldar, *Int. J. Technol. Manag.* **48**, 423 (2009).
- [3] H. K. Onnes, in *Communications from the Physical Laboratory of the University of Leiden* (University of Leiden, Leiden, 1912).
- [4] R. Bhattacharya and M. P. Paranthaman, *High Temperature Superconductors* (Wiley-VCH Verlag GmbH and Co. KGaA, 2006), p. 100.
- [5] P. Mele, K. Prassides, C. Tarantini, A. Palau, P. Badica, A. K. Jha, and T. Endo, *Superconductivity: From Materials Science to Practical Applications* (Springer Nature, New York, 2019).
- [6] J. F. Annett, *Superconductivity, Superfluids and Condensates* (Oxford University Press, Oxford, 2004).
- [7] W. Meissner and R. Ochsenfeld, *Naturwissenschaften* **21**, 787 (1933).
- [8] A. A. Abrikosov, *Zh. Eksp. Teor. Fiz.* **32**, 1442 (1957) [*Sov. Phys. JETP* **5**, 1174 (1957)].
- [9] G. Blatter, M. V. Feigel'man, V. B. Geshkenbein, A. I. Larkin, and V. M. Vinokur, *Rev. Mod. Phys.* **66**, 1125 (1994).
- [10] P. Fulde and R. A. Ferrell, *Phys. Rev.* **135**, A550 (1964).
- [11] A. I. Larkin and Y. N. Ovchinnikov, *Zh. Eksp. Teor. Fiz.* **47**, 1136 (1964) [*Sov. Phys. JETP* **20**, 762 (1965)].
- [12] J. Bardeen, L. N. Cooper, and J. R. Schrieffer, *Phys. Rev.* **108**, 1175 (1957).
- [13] J. J. Kinnunen, J. E. Baarsma, J.-P. Martikainen, and P. Törmä, *Rep. Prog. Phys.* **81**, 046401 (2018).
- [14] D. F. Agterberg, J. S. Davis, S. D. Edkins, E. Fradkin, D. J. Van Harlingen, S. A. Kivelson, P. A. Lee, L. Radzihovsky, J. M. Tranquada, and Y. Wang, *Annu. Rev. Condens. Matter Phys.* **11**, 231 (2020).
- [15] M. Fujita, H. Goka, K. Yamada, J. M. Tranquada, and L. P. Regnault, *Phys. Rev. B* **70**, 104517 (2004).
- [16] A. Bianchi, R. Movshovich, C. Capan, P. G. Pagliuso, and J. L. Sarrao, *Phys. Rev. Lett.* **91**, 187004 (2003).
- [17] R. Lortz, Y. Wang, A. Demuer, P. H. M. Böttger, B. Bergk, G. Zwicknagl, Y. Nakazawa, and J. Wosnitza, *Phys. Rev. Lett.* **99**, 187002 (2007).
- [18] D. F. Agterberg and K. Yang, *J. Phys.: Condens. Matter* **13**, 9259 (2001).
- [19] Q. Wang, C.-R. Hu, and C.-S. Ting, *Phys. Rev. B* **75**, 184515 (2007).
- [20] X.-J. Zuo and C.-D. Gong, *Europhys. Lett.* **86**, 47004 (2009).
- [21] I. Bloch, J. Dalibard, and W. Zwerger, *Rev. Mod. Phys.* **80**, 885 (2008).
- [22] K. B. Davis, M. O. Mewes, M. R. Andrews, N. J. van Druten, D. S. Durfee, D. M. Kurn, and W. Ketterle, *Phys. Rev. Lett.* **75**, 3969 (1995).
- [23] M. Greiner, O. Mandel, T. Esslinger, T. W. Hänsch, and I. Bloch, *Nature (London)* **415**, 39 (2002).
- [24] P. Lecheminant, E. Boulat, and P. Azaria, *Phys. Rev. Lett.* **95**, 240402 (2005).
- [25] J. K. Chin, D. E. Miller, Y. Liu, C. Stan, W. Setiawan, C. Sanner, K. Xu, and W. Ketterle, *Nature (London)* **443**, 961 (2006).
- [26] P. Cladé, C. Ryu, A. Ramanathan, K. Helmerson, and W. D. Phillips, *Phys. Rev. Lett.* **102**, 170401 (2009).
- [27] R. Desbuquois, L. Chomaz, T. Yefsah, J. Léonard, J. Beugnon, C. Weitenberg, and J. Dalibard, *Nat. Phys.* **8**, 645 (2012).
- [28] C. Chin, R. Grimm, P. Julienne, and E. Tiesinga, *Rev. Mod. Phys.* **82**, 1225 (2010).
- [29] V. Galitski and I. B. Spielman, *Nature (London)* **494**, 49 (2013).
- [30] H. Zhai, *Rep. Prog. Phys.* **78**, 026001 (2015).
- [31] T. Esslinger, *Annu. Rev. Condens. Matter Phys.* **1**, 129 (2010).
- [32] Y.-A. Liao, A. S. C. Rittner, T. Paprotta, W. Li, G. B. Partridge, R. G. Hulet, S. K. Baur, and E. J. Mueller, *Nature (London)* **467**, 567 (2010).
- [33] A. E. Feiguin and F. Heidrich-Meisner, *Phys. Rev. B* **76**, 220508(R) (2007).
- [34] A. E. Feiguin, F. Heidrich-Meisner, G. Orso, and W. Zwerger, BCS-BEC crossover and unconventional superfluid order in one dimension, in *The BCS-BEC Crossover and the Unitary Fermi Gas* (Springer, Berlin, 2012), pp. 503–532.
- [35] C. Qu, M. Gong, and C. Zhang, *Phys. Rev. A* **89**, 053618 (2014).
- [36] A. Ptok, A. Cichy, and T. Domański, *J. Phys.: Condens. Matter* **30**, 355602 (2018).
- [37] J. Ruhman, E. Berg, and E. Altman, *Phys. Rev. Lett.* **114**, 100401 (2015).
- [38] J. Ruhman and E. Altman, *Phys. Rev. B* **96**, 085133 (2017).
- [39] A. Lüscher, R. M. Noack, and A. M. Läuchli, *Phys. Rev. A* **78**, 013637 (2008).
- [40] K. Yang, *Phys. Rev. B* **63**, 140511(R) (2001).
- [41] M. Rizzi, M. Polini, M. A. Cazalilla, M. R. Bakhtiari, M. P. Tosi, and R. Fazio, *Phys. Rev. B* **77**, 245105 (2008).
- [42] A. Gelfert and W. Nolting, *J. Phys.: Condens. Matter* **13**, R505 (2001).
- [43] A. Y. Kitaev, *Phys.-Usp.* **44**, 131 (2001).
- [44] S. R. White, *Phys. Rep.* **301**, 187 (1998).
- [45] K. A. Hallberg, *Adv. Phys.* **55**, 477 (2006).
- [46] U. Schollwöck, *Rev. Mod. Phys.* **77**, 259 (2005).
- [47] U. Schollwöck, *Ann. Phys.* **326**, 96 (2011), January 2011 Special Issue.
- [48] S. K. Saha, M. S. Roy, M. Kumar, and Z. G. Soos, *Phys. Rev. B* **101**, 054411 (2020).
- [49] S. K. Saha, D. Maiti, M. Kumar, and Z. G. Soos, *J. Magn. Magn. Mater.* **552**, 169150 (2022).
- [50] D. Dey, A. Parvej, S. Das, S. K. Saha, M. Kumar, S. Ramasesha, and Z. G. Soos, *J. Chem. Sci.* **135**, 25 (2023).
- [51] M. Singh Roy, M. Kumar, J. D. Sau, and S. Tewari, *Phys. Rev. B* **102**, 125135 (2020).
- [52] J. Liang, X. Zhou, P. H. Chui, K. Zhang, S.-J. Gu, M. Gong, G. Chen, and S. Jia, *Sci. Rep.* **5**, 14863 (2015).